Published in final edited form as:
Chem Sci. 2011 June ; 2(6): 1103–1110. doi:10.1039/C1SC00041A.

Cell-compatible, integrin-targeted cryptophane-^{129}Xe NMR biosensors†

Garry K. Seward, **Yubin Bai**, **Najat S. Khan**, and **Ivan J. Dmochowski**
University of Pennsylvania, Department of Chemistry, 231 South 34th St, Philadelphia, PA 19104-6323, USA

Ivan J. Dmochowski: ivandmo@sas.upenn.edu

Abstract

Peptide-modified cryptophane enables sensitive detection of protein analytes using hyperpolarized ^{129}Xe NMR spectroscopy. Here we report improved targeting and delivery of cryptophane to cells expressing $\alpha_v\beta_3$ integrin receptor, which is overexpressed in many human cancers. Cryptophane was functionalized with cyclic RGDyK peptide and Alexa Fluor 488 dye, and cellular internalization was monitored by confocal laser scanning microscopy. Competitive blocking assays confirmed cryptophane endocytosis through an $\alpha_v\beta_3$ integrin receptor-mediated pathway. The peptide–cryptophane conjugate was determined to be nontoxic in normal human lung fibroblasts by MTT assay at the micromolar cryptophane concentrations typically used for hyperpolarized ^{129}Xe NMR biosensing experiments. Flow cytometry revealed 4-fold higher cellular internalization in cancer cells overexpressing the integrin receptor compared to normal cells. Nanomolar inhibitory concentrations (IC_{50} = 20–30 nM) were measured for cryptophane biosensors against vitronectin binding to $\alpha_v\beta_3$ integrin and fibrinogen binding to $\alpha_{IIb}\beta_3$ integrin. Functionalization of the conjugate with two propionic acid groups improved water solubility for hyperpolarized ^{129}Xe NMR spectroscopic studies, which revealed a single resonance at 67 ppm for the ^{129}Xe-cryptophane–cyclic RGDyK biosensor. Introduction of $\alpha_{IIb}\beta_3$ integrin receptor in detergent solution generated a new “bound” ^{129}Xe biosensor peak that was shifted 4 ppm downfield from the “free” ^{129}Xe biosensor.

Introduction

Very early-stage detection of cancer in humans by magnetic resonance imaging (MRI) will require new contrast agents with greater sensitivity and molecular specificity. MRI allows non-invasive imaging of buried tissue using non-ionizing radiation, and typically involves the detection of abundant proton signals from water and fat. Lacking are specific molecular signatures for cancer biomarkers that could be employed for diagnostic purposes. Promising alternate nuclei include ^{129}Xe, ^{13}C, and ^{3}He, which can be hyperpolarized to generate fairly long-lived, non-Boltzmann distributions of nuclear spins, with large magnetic resonance

†Electronic supplementary information (ESI) available: Reagents list, general characterization methods, synthesis of azido-Lys peptide, cell culture, HPLC traces, flow cytometry, fluorescence data, and hyperpolarized ^{129}Xe NMR spectrum. See DOI: 10.1039/c1sc00041a

Correspondence to: Ivan J. Dmochowski, ivandmo@sas.upenn.edu.

signals. These hyperpolarized nuclei enable physiological assays,[1] and provide more sensitive MRI methods for studying proteins and metabolites than standard gadolinium chelates or iron oxide nanoparticles.[2–4] ^{129}Xe is particularly attractive as it is inert, has a more than 200-ppm chemical shift window in aqueous solutions, and can be hyperpolarized *via* optical pumping to enhance ^{129}Xe nuclear magnetic resonance (NMR) signals by more than 10 000-fold.[5]

Importantly, the responsiveness of ^{129}Xe NMR chemical shifts to the molecular environment allows the simultaneous detection of multiple species in solution. The ability to achieve ‘multiplexed’ detection of rare biomarkers would facilitate the early and accurate diagnosis of cancer and many other diseases.

Xenon exhibits significant affinity for organic cavitands such as cryptophane,[6] calixarene[7,8] and cucurbit[6]uril.[9] Most widely investigated with xenon is cryptophane-A,[6] which is composed of three ethylene linkers joining two cyclotriguaiacylene units and has an internal cavity volume ~90 Å^3.[10] A tricarboxylate-functionalized cryptophane-A derivative showed exceptional affinity for xenon in both water (K_A = 30 000 M^{-1}) and human plasma (K_A = 22 000 M^{-1}) at 37 °C.[11] Importantly, cryptophane-A has been used to generate biosensors that exploit xenon’s physical properties to monitor biological activity by laser-polarized ^{129}Xe NMR spectroscopy.[12,13] For example, biotin-functionalized cryptophanes produced a 1–4 ppm change in ^{129}Xe NMR chemical shift upon streptavidin binding. [13–15] More recently, a series of benzenesulfonamide-functionalized cryptophanes produced 3.0–7.5 ppm downfield shifts upon binding to carbonic anhydrase I or II.[16] Improvements in xenon hyperpolarization technology[17] and Hyper-CEST NMR[18] remote detection strategies[19] have also led to significant gains in detection sensitivity. In a recent example, MS2 viral capsid modified with 125 cryptophane molecules was detected at concentrations as low as 0.7 picomolar.[20]

A particular focus of our lab has been the design of xenon biosensors for the early and accurate diagnosis of cancer.[21] Towards this goal, cryptophane biosensors targeting matrix metalloproteinase, carbonic anhydrase, and integrin cancer biomarkers were previously synthesized.[12,16,22,23] The current study provides strong evidence that cryptophane–peptide conjugates can be targeted specifically to cells that overexpress the $\alpha_v\beta_3$ integrin receptor. Integrin $\alpha_v\beta_3$ is a heterodimeric cell adhesion protein that has been linked to both tumor angiogenesis and metastasis.[24,25] The $\alpha_v\beta_3$ integrin receptor is also known to be highly up-regulated in a wide range of fast growing tumor cells, compared to minimal expression in most normal tissues, making it a broad spectrum tumor marker.[26–28] Peptides containing arginine–glycine–aspartic acid (RGD) sequences are known to bind the integrin receptor with high affinity (IC_{50} = 29 nM against ^{125}I-echistatin, an RGD-containing snake venom peptide).[29–32] Probes containing multimeric or monomeric RGD peptides have been used to image $\alpha_v\beta_3$ integrin receptor expression by fluorescence,[33] MRI,[28,34] and nuclear imaging techniques.[35,36] In our previous study, cryptophane was targeted to cell surface integrin receptors by conjugation to a linear $(RGD)_4$ peptide.[23] The cryptophane–$(RGD)_4$ conjugate exhibited limited water solubility, likely due to intermolecular electrostatic interactions and hydrogen bonding between arginine and aspartic acid residues. This necessitated use of 10%

dimethyl sulfoxide for water solubilization, and limited the range of analytical and cell characterization studies that could be performed with the cryptophane–$(RGD)_4$ biosensor.[23]

Herein we describe the use of a cyclic targeting peptide, c[RGDyK], to deliver cryptophane specifically to cells expressing $\alpha_v\beta_3$ integrin receptor. While the linear RGD tetra repeat effectively binds integrin receptors, cyclic RGD peptides are known to target $\alpha_v\beta_3$ integrin receptors with approximately 10-fold higher affinity.[33] By employing a peptide ligand with higher binding affinity, the cryptophane biosensor was more effectively delivered to $\alpha_v\beta_3$ integrin-expressing cells. The c[RGDyK]-labeled cryptophane was further modified to improve water solubility and allow detection of integrin receptor by hyperpolarized ^{129}Xe NMR spectroscopy.

Results and discussion

Synthesis of cryptophane biosensors

The synthesis of cryptophane biosensor **3** is shown in Scheme 1. Tripropargylated cryptophane **1** was synthesized as previously reported with yields of 2–4%.[11,16] The amine of the lysine side chain in the c[RGDyK] peptide was converted to azidopeptide **2** in greater than 95% yield by overnight reaction with triflyl azide in water, CH_2Cl_2 and methanol (1:1:1).[37] The azidopeptide was then reacted with **1** by a copper(I)-catalyzed [3 + 2] azide–alkyne Huisgen cycloaddition in 80–89% yield[38–41] and the product was purified by reverse-phase HPLC. HPLC purification indicated the presence of two side-products that correspond to cryptophane conjugated to two or three peptides. These adducts were readily separated from biosensor **3** during HPLC purification, allowing isolation of the desired mono-functionalized product.

Biosensor **3** required addition of 150 mM NaCl to be dissolved in aqueous solution, suggesting aggregation due to an interaction between the charged residues of the c[RGDyK] peptide. Evidence of aggregation was seen at concentrations of **3** as low as 120 μM by UV-vis spectroscopy. For ^{129}Xe NMR studies, two azidopropionic acids were reacted in 80% yield with the remaining propargyl moieties of **3** to generate biosensor **5**. Biosensor **5** was soluble in pure water at concentrations of up to 250 μM, indicating a substantial improvement in water solubility.

In vitro competitive binding assay

The binding of biosensor **3** was assessed by *in vitro* competitive binding assays (Scheme 2) against $\alpha_{IIb}\beta_3$, $\alpha_v\beta_3$ and $\alpha_v\beta_5$ integrin receptors to investigate cell receptor targeting. The resulting IC_{50} values are shown in Table 1. IC_{50} values for cyclic RAD and RGD peptides are comparable to previously reported values for these peptides binding integrins assayed by this method.[42,43] When the inhibition of vitronectin binding to immobilized $a_v\beta_3$ integrin receptor was examined, the IC_{50} value for biosensor **3** was found to be 32 nM. Compared to the c[RGDyK] peptide alone, which had an IC_{50} of 8 nM, biosensor **3** bound with approximately 4-fold lower affinity.

Inhibition of fibrinogen binding to $\alpha_{IIb}\beta_3$ was also measured for **3** and the IC_{50} value was found to be 18 nM. This reflects approximately 10-fold weaker binding for this receptor

compared to the c[RGDyK] peptide (IC_{50} = 1.6 nM). IC_{50} values for both $\alpha_{IIb}\beta_3$ and $\alpha_v\beta_3$ integrin proteins represent tight binding and should allow for receptor targeting during *in vitro* experiments.

Binding was also assessed for $\alpha_v\beta_5$ integrin receptor as it is sometimes co-expressed in tumors and can contribute to angiogenesis but is not known to bind RGD motifs.[43,44] Notably little binding was observed in these binding assays. The c[RGDyK] peptide bound with an IC_{50} of 200 nM, while the biosensor bound with IC_{50} of 700 nM, indicating a high degree of specificity of biosensor **3** for $\alpha_v\beta_3$ integrin receptors.

Viability studies

Cell viability for **3** was measured by MTT assays in NCI-H1975 lung carcinoma cells, AsPC-1 pancreatic carcinoma and HFL-1 lung fibroblasts after 24 h exposure to increasing concentrations of **3**, as shown in Fig. 1. Viability was reduced by 50% at a cryptophane concentration between 75 and 100 μM in AsPC-1 and NCI-H1975 cell cultures. The biosensor showed lowest toxicity in the HFL-1 cell line. A 50% reduction in viability was not observed in HFL-1 fibroblasts, indicating minimal toxicity in normal human cells at the concentrations of interest for performing ^{129}Xe NMR biosensing experiments. Increased cytotoxicity in AsPC-1 and NCI-H1975 cell cultures was likely due to higher expression levels of $\alpha_v\beta_3$ integrin receptors in cancer cell lines,[29,30] leading to increased cellular uptake of cryptophane. Maximum toxicity was found to be 61% in AsPC-1 and 57% in NCI-H1975 cells with 100 μM biosensor **3**. These toxicity values are in agreement with previously measured cell-permeable cryptophanes.[23] In a previous study we found that when a linear RGD peptide was attached to cryptophane and tested in cells, maximum toxicity was in the range of 30–40% in both cancerous and non-cancerous cells after 24 h incubation at 100 μM concentration.[23] Biosensor 3 was similarly toxic in the non-cancerous HFL-1 fibroblasts, reaching a maximum toxicity of 40% after 24 h incubation at 100 μM concentration.

Cellular uptake

Uptake of Alexa Fluor 488-labeled c[RGDyK]-cryptophane **4** by cells was monitored by confocal laser scanning microscopy (Fig. 2). Incubation of AsPC-1 (Fig. 2A) and HFL-1 (Fig. 2E) cells with **4** (1 μM) for 1 h gave bright fluorescence throughout the cell interior. When cells were co-incubated with **4** and a 10-fold excess of c[RADfK] peptide (which is known to be a weak binder of the $\alpha_v\beta_3$ integrin receptor), levels of fluorescence remained throughout the cell interior (Fig. 2B and 2F). From confocal images, cellular fluorescence was observed to decrease significantly when **4** was co-incubated with a 10-fold excess of either c[RGDyK] peptide (Fig. 2C and 2G) or anti-α_v antibody (Fig. 2D and 2H), both of which target $\alpha_v\beta_3$ integrin receptor with high affinity. Both the antibody and peptide control blocked cryptophane biosensor binding and inhibited receptor-mediated endocytosis from occurring in these cell lines. These co-incubation studies strongly suggest that the c[RGDyK]-labeled cryptophane is specifically recognized by $\alpha_v\beta_3$ integrin receptor and the $\alpha_v\beta_3$ subunit is necessary for efficient cellular uptake. This also indicates that the water-soluble cryptophane without a targeting moiety is not delivered to cells as no uptake was seen when blocking controls were done. This differs from results obtained with a less water-

soluble dicarboxylic acid cryptophane, which was shown recently to partition from water into suspensions of Intralipid® vesicles.[45]

Cellular internalization of **4** was further confirmed by flow cytometry. As shown in Fig. 3, significant amounts of cell-associated fluorescence were observed after 1 h incubation in both AsPC-1 and HFL-1 cell lines. Fluorescence remained at similar intensities when AsPC-1 and HFL-1 cells were co-incubated with fluorescent biosensor **4** and a 10-fold excess of c[RADfK] peptide. However, when **4** was co-incubated with 10-fold excess of either c[RGDyK] peptide or the anti-α_v antibody, both of which bind integrin protein with high affinity, fluorescence intensities were reduced to background level. Flow cytometry also confirmed greater internalization of **4** in AsPC-1 cells when compared to HFL-1 cells. Mean fluorescence intensities after incubation with cryptophane were approximately four times higher in AsPC-1 cells than in HFL-1. This higher uptake is attributed to increased expression of the target receptor in cancer cell lines *versus* normal fibroblasts.[29,30] These results were expected as HFL-1 cells are known to have minimal $\alpha_v\beta_3$ integrin receptor expression unless activated by a smooth muscle actin or transforming growth factor β.[46–48]

In our previous study, a linear tetrameric RGD peptide was used to target cryptophane to human fibroblasts and cancer cells expressing $\alpha_v\beta_3$ integrin receptor.[23] Fluorometric quantitation of 100 μL volumes of cell lysate showed that 0.08 nmol of dyelabeled cryptophane was delivered to the cell population over a 24 h incubation period. This led to an estimate of the intracellular cryptophane concentration in the range of 100–160 μM. In the present study, **4** showed higher uptake after a shorter 1.5 h incubation, achieving 990 nM in cell lysates, which corresponds to delivery of about 0.1 nmol of **4** into live cells. In this case, it was possible to determine the concentration of dye label by UV-vis spectroscopy. Additionally, after 3 h incubation the concentration in the cell lysate solution increased to 1.5 μM. The average volume of the cell was calculated based on the diameter of AsPC-1 cells in suspension (~40 microns), and the fraction of the 100 μL lysate solution volume originally occupied by AsPC-1 cells was found to be 0.0075. Using these calculations, the intracellular concentration of biosensor **4** was estimated to be in the range of 130–200 μM after 3 h incubation, indicating that a small improvement in cellular delivery was achieved using c[RGDyK] relative to the previously studied $(RGD)_4$ peptide.[23] This was likely due to the higher binding affinity of c[RGDyK] relative to $(RGD)_4$ for $\alpha_v\beta_3$ integrin cell surface receptors.

Hyperpolarized ^{129}Xe NMR studies

To improve cryptophane solubility, and achieve concentrations useful for ^{129}Xe NMR studies, the two remaining propargyl groups on biosensor 3 were reacted with azidopropionic acid by an additional [3 + 2] cycloaddition reaction, yielding **5.** The propionic acid groups conferred substantial gains in solubility, allowing the collection of a hyperpolarized ^{129}Xe NMR spectrum in PBS buffer. Hyperpolarized ^{129}Xe NMR spectra of compound **5** were acquired in three different solutions. Fig. 4a shows **5** (100 μM) dissolved in Tris buffer (1 mM, pH 7.2), which gave a ^{129}Xe NMR chemical shift at 65.8 ppm. The two enantiomers of 5 produced just one ^{129}Xe NMR resonance with a line width of 80 Hz (0.57 ppm), which is similar to results we obtained with previous cryptophane biosensors.[16]

In Fig. 4b, 5 (50 μM) and $\alpha_{IIb}\beta_3$ integrin (16 μM) were mixed in Tris buffer (1 mM, pH 7.2) with 30% glycerol and 0.1% Triton X-100. The $\alpha_{IIb}\beta_3$ integrin was chosen instead of $\alpha_v\beta_3$ integrin, due to the relative ease of isolating and lower cost of purchasing milligram quantities of this protein. Keeping the $\alpha_{IIb}\beta_3$ integrin membrane protein in solution required addition of glycerol and Triton X-100, and glycerol also mitigated foaming while introducing xenon gas. “Free” cryptophane gave a ^{129}Xe NMR peak at 67.1 ppm, while “bound” cryptophane appeared at 71.2 ppm, representing a 4.1 ppm downfield shift. Signal-to-noise ratio for the single “bound” cryptophane–protein peak was ~3:1. With the racemic mixture of biosensors, protein binding results inevitably in diastereomers, which in some cases can produce multiple “bound” ^{129}Xe NMR peaks. We have seen single “bound” peaks previously in cases where the cryptophane enantiomers are constrained near the protein target surface, and the xenon by chance senses the environment identically inside both biosensors.[16] The short alkyl spacer for c[RGDyK] peptide in **5** may similarly tether both cryptophane biosensor racemates at the integrin receptor, effectively creating one xenon binding site. Alternatively, a second peak corresponding to the other diastereomer may reside under the “free” peak (~67 ppm).

The NMR binding assay described above was constrained by a number of experimental factors. The concentrations were selected to achieve a balance between the detection limit of our current ^{129}Xe NMR data collection method and the well documented aggregation behavior of this integrin protein. Integrin protein aggregates at concentrations greater than 9 μM in solution without detergent, thus we limited experiments to 16–20 μM integrin receptor with detergent.[49,50] Another reason for the “bound” signal being weak is the broad line width compared to some xenon biosensors bound to other protein targets (avidin, 0.15 ppm; carbonic anhydrase I and II, 0.19–0.27 ppm[16]). In other cases, it has been observed that “bound” peaks for many xenon biosensors are considerably broadened (10–30 Hz to 100–150 Hz,[14] and even 1–5 kHz[20]). Although peak broadening tends to be an obstacle in identifying peaks in high-resolution NMR spectra, this problem will be mitigated in a saturation transfer scheme (Hyper-CEST).[18] Given that we observe a 4 ppm chemical shift change upon integrin binding, the “bound” and “free” peaks can be selectively saturated easily. This change in chemical shift is comparable to our previous carbonic anhydrase biosensor work (3.0–7.5 ppm)[16] and a biosensor optimization study with biotin–avidin (3–4 ppm).[14] Considerably smaller ^{129}Xe NMR chemical shifts were observed in two related protein-binding studies (biotin–avidin, ~1 ppm;[13] major histocompatibility complex, ~1 ppm[51]).

To make a competition assay (Fig. 4c), c[RGDyK] (100 μM) was added to a fresh solution (1 mM Tris buffer, pH 7.2; 30% glycerol and 0.1% Triton X-100) containing biosensor **5** (100 μM) and $\alpha_{IIb}\beta_3$ integrin (20 μM). Here “free” cryptophane gave the same ^{129}Xe NMR chemical shift, and no “bound” cryptophane was detected, which indicated that the peptide blocked **5** from binding to $\alpha_{IIb}\beta_3$ integrin. The disappearance of the smaller “bound” peak after addition of the competing peptide further confirmed that the spectral change observed upon addition of $\alpha_{IIb}\beta_3$ is due to protein binding by the cryptophane biosensor.

Conclusions

This work represents the first in-depth investigation of a xenon NMR biosensor binding to proteins that are well recognized cancer biomarkers and cell surface receptors. As such, we were forced to confront challenges of poor solubility and aggregation behavior involving both the integrin receptor and the biosensor itself. We worked to engineer specific molecular interactions with the $\alpha_v\beta_3$ integrin cancer biomarker and distinguish cancer cells from healthy cells based on cell uptake properties. This work was accomplished by conjugating the $\alpha_v\beta_3$ integrin receptor-targeting peptide c[RGDyK] to a tripropargyl derivative of cryptophane-A *via* a [3 + 2] cycloaddition reaction. This biosensor (3) was found to bind $\alpha_v\beta_3$ and $\alpha_{IIb}\beta_3$ integrin receptor proteins with the expected nanomolar affinity (IC_{50} = 20–30 nM), thus ensuring the possibility of cell receptor targeting. The *in vitro* integrin competitive binding assay confirmed that the cryptophane had little effect on integrin receptor binding. Cryptophane was found to be only moderately toxic to normal lung fibroblasts at relevant biosensing concentrations although 50% viability was reached in the cancer cell lines studied at concentrations of 75–100 μM.

Biosensor **4**, labeled with Alexa Fluor 488, was useful for fluorescence microscopy and flow cytometry experiments. These studies confirmed that cryptophane was specifically targeted and delivered into cells by an $\alpha_v\beta_3$ integrin receptor-mediated pathway. Quantification of cellular delivery indicated that internalization occurs at concentrations suitable for hyper-polarized ^{129}Xe NMR studies. Most importantly, internalization was notably higher in AsPC-1 cancer cells compared to fibroblasts from the human lung, suggesting potential for targeted delivery of cryptophanes in future *in vivo* studies.

To perform successful ^{129}Xe magnetic resonance experiments two propionic acid groups were added to **3**, generating biosensor **5** with greatly increased cryptophane solubility in aqueous media. Upon binding to the $\alpha_{IIb}\beta_3$ integrin receptor, the hyper-polarized ^{129}Xe NMR chemical shift showed a change of about 4 ppm downfield. This chemical shift change is comparable to results we obtained previously with xenon biosensors targeting human carbonic anhydrase I and II,[16,22] and represents one of the largest protein-mediated ^{129}Xe NMR chemical shift changes observed to date. Having demonstrated the compatibility of xenon biosensors with cells and the ability to target specific protein receptors and achieve large hyperpolarized ^{129}Xe NMR chemical shift changes, these studies pave the way for cellular spectroscopy and imaging experiments.

Experimental

Synthesis of peptide–cryptophane conjugate 3 and fluorescently labeled conjugate 4

A [3 + 2] cycloaddition reaction between azide-functionalized c[RGDyK] peptide and tripropargyl cryptophane **1** was performed to generate the mono-functionalized peptide–cryptophane conjugate **3** (Scheme 1) following a previously reported protocol.[12] The tripropargylated derivative of cryptophane-A **1** was synthesized as previously described.[11,16] Tripropargyl cryptophane **1** (37.3 mg, 0.0390 mmol) was dissolved in DMSO. An aqueous solution of copper(II) sulfate (0.6 mg, 0.004 mmol, 0.1 equiv.) was added to the solution, followed by the addition of azidopeptide **2** (25.0 mg, 0.0390 mmol, 1.0 equiv.), 2,6-lutidine

(0.8 mg, 0.007 mmol, 0.2 equiv.) and sodium ascorbate (344.0 mg, 1.737 mmol, 45 equiv.). The suspension was degassed with N_2 and stirred at r.t. overnight. The reaction mixture was passaged through a 0.22 micron filter. Confirmation of the reaction was obtained by analytical HPLC using a gradient: time 0, A/B = 85/15; 0–45 min, linear increase to A/B = 40/60; time 45–47 min, linear change to A/B = 20/80. Biosensor **3** was purified by semi-preparative HPLC as shown in the supporting information (Figure S2).† The extinction coefficient for **3** at 280 nm was determined: ε_{280} = 13 400 M^{-1} cm^{-1}. MALDI MS ($C_{87}H_{95}N_{11}O_{20}$) [M + H^+]: calcd, 1614.74; found, 1616.60.

Biosensor **3** was reacted with Alexa Fluor 488 azide by a [3 + 2] azide–alkyne cycloaddition to give fluorescently labeled biosensor **4**, following the manufacturer protocol. Analytical HPLC was performed using a gradient: time 0, A/B = 85/15; 0–45 min, linear increase to A/B = 40/60; time 45–47 min, linear change to A/B = 20/80. Semi-preparative HPLC was performed as shown in the supporting information (Figure S3).† Dye conjugation was determined to occur in 85% yield, based on the absorbances measured at 494 nm (ε_{494} = 71 000 M^{-1} cm^{-1}) and 280 nm (ε_{280} = 21 300 M^{-1} cm^{-1}). MALDI MS ($C_{114}H_{119}N_{17}O_{30}S_2$) [$M$ + H^+]: calcd, 2269.78; found, 2263.06.

Synthesis of c[RGDyK]-cryptophane biosensor 5 with improved water solubility

The c[RGDyK]-conjugated cryptophane **3** was reacted with azidopropionic acid to generate a more water-soluble biosensor **5** for ^{129}Xe NMR studies. Azidopropionic acid was generated according to previously reported protocols.[12,16,52] **3** (10.0 mg, 0.00600 mmol) was dissolved in DMSO. To this solution the azidopropionic acid (2.8 mg, 0.024 mmol, 4.0 equiv.) was added followed by the addition of 2,6-lutidine (0.1 mg, 0.001 mmol, 0.2 equiv.), an aqueous solution of copper(II) sulfate (0.003 mmol, 0.5 equiv.), and sodium ascorbate (53.5 mg, 0.270 mmol, 45 equiv.). Reaction progress was monitored by analytical HPLC using a gradient: time 0, A/B = 85/15; 0–45 min, linear increase to A/B = 40/60; time 45–47 min, linear change to A/B = 20/80; 47–57 min, A/B = 20/80. Biosensor **5** was purified by semi-preparative HPLC as shown in Figure S4 in the supporting information.† The extinction coefficient for **5** at 280 nm was determined: ε_{280} = 13 700 M^{-1} cm^{-1}. MALDI MS ($C_{93}H_{104}N_{17}O_{24}$) [$M$ + H^+]: calcd, 1843.92; found, 1845.90.

Cell viability assays

Cells were plated at 10 000 cells per well in 96 well plates and grown overnight at 37 °C. Biosensor **3** was then added from a stock solution in DPBS to wells in triplicate at final concentrations of 2, 10, 25, 50, 75 and 100 μM and incubated for 24 h. The medium was removed and the cells were washed three times with DPBS before being treated with 20 μL of 5.0 mg mL^{-1} MTT solution for 2 h. The medium was removed once more and the resulting crystals were dissolved in DMSO. Absorbance at 540 nm was recorded in each well using the plate reader. Absorbance from wells not containing cells was subtracted as background, and the reduction in cell growth was calculated as a percentage of the absorbance in the absence of any treatment. Data show the mean of at least three independent experiments ± *SD.*

Cell uptake studies by confocal microscopy

Cells were plated at 20 000 cells per well and grown to confluence in LabTek 8-well microscope slides with glass coverslip bottoms. For uptake studies, cells were incubated with 1 μM solutions of Alexa Fluor 488-labeled c[RGDyK] cryptophane **4** for 1 h. For blocking studies, cells were co-incubated for 1 h with a 10 μM solution of c[RGDyK] (blocking) or c[RADfK] (negative control) peptide containing D-phenylalanine in addition to 1 μM **4.** In the antibody blocking studies, cells were co-incubated with 0.15 mg mL^{-1} blocking anti-α_v antibody and 1 μM **4.** To visualize the results, the medium was removed and the cells were washed three times with DPBS before adding DMEM containing no phenol red. Cells were visualized using an Olympus FV1000 confocal laser scanning microscope with 488 nm argon-ion laser excitation and Cy3 emission filter under 40× magnification (Olympus UApo/340 40×, 1.15 W).

Flow cytometry

T-25 cell culture flasks were inoculated with 1.5 million viable cells in RPMI-1640 medium (5 mL) and incubated at 37 °C overnight. Then, the medium was removed and 2 mL of fresh RPMI-1640 was added. **4** (1 μM final concentration) was then added to the flask and incubated for 1 h. For blocking studies cells were co-incubated with 0.15 mg mL^{-1} anti-α_v antibody, 10 μM c[RGDyK] (blocking), or 10 μM c[RADfK] (negative control) for 1 h. The cells were then washed with PBS three times and trypsinized. After centrifugation, the cell pellet was resuspended in a solution of 10% FBS in Dulbecco's PBS, and these cells were analyzed by flow cytometry.

Cellular uptake monitored by UV-vis spectroscopy

AsPC-1 cells were plated in 96 well plates at 10 000 cells per well and incubated overnight at 37 °C. **4** was added to each well at a concentration of 10 μM and placed back in the incubator. After 1.5 h incubation, the cells were removed and rinsed three times with DPBS solution. Triton X-100 solution (0.25%, 100 μL) was then added to lyse the cells and after 20 min the UV-vis absorbance at 494 nm was measured.

Isolation of $\alpha_{IIb}\beta_3$ integrin receptor from human blood platelets

Human blood platelet suspensions were obtained from Joel S. Bennett (UPenn School of Medicine). The $\alpha_{IIb}\beta_3$ integrin protein was isolated from platelets using a modified procedure.[53] Platelets were lysed by rapid nitrogen decompression in a cell bomb, with nitrogen supplied at 1200–1500 psi for 5 min, followed by opening of the release valve. Platelets were collected in 50 mL Falcon tubes and kept on ice. The platelet lysate was then centrifuged at 7000 g for 15 min at 4 °C. The supernatant was decanted and centrifuged at 30,000 g for 1 h at 4 °C. The resulting pellet was resuspended in 0.2% Triton X-100 in Tris buffer (200 mM Tris, 1 mM $MgCl_2$, 1 mM $CaCl_2$, pH 7.2). The resuspended pellet was added to SP Sepharose that had been prewashed with buffer (30 mL) and mixed for 1 h at 4 °C. The unbound fraction was removed and loaded onto prewashed concanavalin A-sepharose 4B resin (Sigma) and mixed for 2 h at 4 °C. The unbound fraction was removed. The bound fraction was eluted with buffer plus 100 mM methyl-α-D-mannopyranoside. Fractions containing protein were pooled and concentrated using Millipore centrifugal filter

units (MWCO, 30 000 Da). Protein purity was analyzed by SDS-PAGE, which showed the presence of two bands with molecular weights of 100 and 120 kDa. These bands corresponded to the α_{IIb} and β_3 subunits, respectively.[53] Isolation yielded 2.5 mg of protein from 300 mL of platelet lysates.

In vitro competitive binding assay

c[RGDyK]-conjugated cryptophane **3** was tested for its ability to inhibit fibrinogen binding to purified human $\alpha_{IIb}\beta_3$ integrin receptor, the attachment of vitronectin to purified $\alpha_v\beta_3$ integrin receptor, and the attachment of fibronectin to $\alpha_v\beta_5$ integrin receptor. Integrin protein was added to 96-well polystyrene microtiter plates at 0.1 μg well^{-1}. After overnight incubation at 4 °C, the plates were washed and then blocked with milk solution at r.t. for 2 h. The blocking buffer was removed, and **3** was added to wells at concentrations from 0.001 nM to 10 μM. Biotinylated fibrinogen, fibronectin or vitronectin solution (0.1 μg well^{-1}) was then added to each well as a standard competitor. The plates were incubated at r.t. for 3 h, washed, and the bound biotinylated substrate was detected using NeutrAvidin-HRP conjugate at 0.01 μg well^{-1} and TMB substrate system. Absorbance at 450 nm was read by a UV-vis plate reader. The concentration of inhibitor producing 50% inhibition (IC_{50}) of fibrinogen or vitronectin binding to integrin protein was calculated using BioDataFit (Chang Biosciences, Castro Valley, CA) with the four parameter Hill Slope model to eqn (1):

$$a+(b-a)/(1+10^{(x-c)d}) \quad (1)$$

where *x* is the concentration of inhibitor, *a* is the minimum horseradish peroxidase activity, *b* is the maximum horseradish peroxidase activity, *c* is the IC_{50} concentration and *d* is the Hill coefficient. The c[RGDyK] and c[RADfK] peptides were also tested for inhibition and the data fit using the same methods.

Hyperpolarized ^{129}Xe NMR spectroscopy

Hyperpolarized ^{129}Xe was generated using a home-built ^{129}Xe hyperpolarizer, which is based on the formerly commercially available Nycomed-Amersham (now GE) IGI.Xe.2000 system. A gas mixture of 89% N_2, 10% He, and 1% natural abundance Xe (Spectra Gases) was flowed through the hyperpolarizer. ^{129}Xe was hyperpolarized to 10–15% after cryogenically separated, accumulated, thawed, and collected in CAV NMR tubes (New Era). After Xe collection, NMR tubes were shaken vigorously to mix cryptophane solutions with Xe.

All ^{129}Xe NMR measurements were carried out on a 500 MHz Bruker BioDRX NMR spectrometer. RF pulse frequency for ^{129}Xe was 138.12 MHz. Samples were observed using either a 5 mm PABBO NMR probe or a similar 10 mm probe.

^{129}Xe NMR spectra were acquired using the exchange signal averaging (ESA) method.[54] Selective pulses (90° flip angle, EBurp1 shaped) were generated at the Xe@cryptophane resonance frequencies. Each pulse lasted 5 ms, which gave a designated excitation region ~1 kHz (~7.2 ppm). All spectra were signal averaged by 40 scans. A delay of 0.15 s was given between scans to allow polarized Xe to exchange in and depolarized Xe to exchange out of

the cryptophane cavity. The natural line widths of Xe@cryptophane peaks are around 80 Hz (FWHM, Lorentzian fitted). The spectra shown above are exponentially broadened by 100 Hz, to give larger signal/noise ratio. Sample temperature was controlled by VT unit on NMR spectrometer to 27 ± 1 °C.

Supplementary Material

Refer to Web version on PubMed Central for supplementary material.

Acknowledgments

We thank Scott Diamond for access to the 2102 Envision Multilabel Microplate Reader and Bill Degrado and Joel Bennett for help with isolating $\alpha_{IIb}\beta_3$ integrin. This work was supported by NIH CA110104 and DOD BC061527.

Notes and references

1. Branca RT, Cleveland ZI, Fubara B, Kumar CSSR, Maronpot RR, Leuschner C, Warren WS, Driehuys B. Proc Natl Acad Sci U S A. 2010; 107:3693–3697. [PubMed: 20142483]
2. Golman K, Zandt RI, Lerche M, Pehrson R, Ardenkjaer-Larsen JH. Cancer Res. 2006; 66:10855–10860. [PubMed: 17108122]
3. Mugler JP, Driehuys B, Brookeman JR, Cates GD, Berr SS, Bryant RG, Daniel TM, de Lange EE, Downs JH 3rd, Erickson CJ, Happer W, Hinton DP, Kassel NF, Maier T, Phillips CD, Saam BT, Sauer KL, Wagshul ME. Magn Reson Med. 1997; 37:809–815. [PubMed: 9178229]
4. Hopkins SR, Levin DL, Emami K, Kadlecek S, Yu J, Ishii M, Rizi RR. J Appl Physiol. 2007; 102:1244–1254. [PubMed: 17158249]
5. Berthault P, Huber G, Desvaux H. Prog Nucl Magn Reson Spectrosc. 2009; 55:35–60.
6. Brotin T, Dutasta JP. Chem Rev. 2009; 109:88–130. [PubMed: 19086781]
7. Brouwer EB, Enright GD, Ripmeester JA. Chem Commun. 1997:939–940.
8. Enright GD, Udachin KA, Moudrakovski IL, Ripmeester JA. J Am Chem Soc. 2003; 125:9896–9897. [PubMed: 12914432]
9. Miyahara Y, Abe K, Inazu T. Angew Chem Int Ed. 2002; 41:3020–3023.
10. Taratula O, Hill PA, Khan NS, Carroll PJ, Dmochowski IJ. Nat Commun. 2010; 1:148. [PubMed: 21266998]
11. Hill PA, Wei Q, Eckenhoff RG, Dmochowski IJ. J Am Chem Soc. 2007; 129:9262–9263. [PubMed: 17616197]
12. Wei Q, Seward GK, Hill PA, Patton B, Dimitrov IE, Kuzma NN, Dmochowski IJ. J Am Chem Soc. 2006; 128:13274–13283. [PubMed: 17017809]
13. Spence MM, Rubin SM, Dimitrov IE, Ruiz EJ, Wemmer DE, Pines A, Yao SQ, Tian F, Schultz PG. Proc Natl Acad Sci U S A. 2001; 98:10654–10657. [PubMed: 11535830]
14. Lowery TJ, Garcia S, Chavez L, Ruiz EJ, Wu T, Brotin T, Dutasta JP, King DS, Schultz PG, Pines A, Wemmer DE. ChemBio Chem. 2006; 7:65–73.
15. Hilty C, Lowery TJ, Wemmer DE, Pines A. Angew Chem Int Ed. 2006; 45:70–73.
16. Chambers JM, Hill PA, Aaron JA, Han Z, Christianson DW, Kuzma NN, Dmochowski IJ. J Am Chem Soc. 2009; 131:563–569. [PubMed: 19140795]
17. Hersman FW, Ruset IC, Ketel S, Muradian I, Covrig SD, Distelbrink J, Porter W, Watt D, Ketel J, Brackett J, Hope A, Patz S. Acad Radiol. 2008; 15:683–692. [PubMed: 18486005]
18. Schroder L, Lowery TJ, Hilty C, Wemmer DE, Pines A. Science. 2006; 314:446–449. [PubMed: 17053143]
19. Moulé AJ, Spence MM, Han SI, Seeley JA, Pierce KL, Saxena S, Pines A. Proc Natl Acad Sci U S A. 2003; 100:9122–9127. [PubMed: 12876195]
20. Meldrum T, Seim KL, Bajaj VS, Palaniappan KK, Wu W, Francis MB, Wemmer DE, Pines A. J Am Chem Soc. 2010; 132:5936–5937. [PubMed: 20392049]

21. Taratula O, Dmochowski IJ. Curr Opin Chem Biol. 2010; 14:97–104. [PubMed: 19914122]
22. Aaron JA, Chambers JM, Jude KM, Di Costanzo L, Dmochowski IJ, Christianson DW. J Am Chem Soc. 2008; 130:6942–6943. [PubMed: 18461940]
23. Seward GK, Wei Q, Dmochowski IJ. Bioconjugate Chem. 2008; 19:2129–2135.
24. Byzova TV, Goldman CK, Pampori N, Thomas KA, Bett A, Shattil SJ, Plow EF. Mol Cell. 2000; 6:851–860. [PubMed: 11090623]
25. Byzova TV, Kim W, Midura RJ, Plow EF. Exp Cell Res. 2000; 254:299–308. [PubMed: 10640428]
26. Cairns RA, Khokha R, Hill RP. Curr Mol Med. 2003; 3:659–671. [PubMed: 14601640]
27. Felding-Habermann B. Clin Exp Metastasis. 2003; 20:203–213. [PubMed: 12741679]
28. Cai W, Chen X. J Nucl Med. 2008; 49(Suppl. 2):113S–128S. [PubMed: 18523069]
29. Pierschbacher MD, Hayman EG, Ruoslahti E. J Cell Biochem. 1985; 28:115–126. [PubMed: 3908463]
30. Pierschbacher MD, Ruoslahti E. Nature. 1984; 309:30–33. [PubMed: 6325925]
31. Ruoslahti E. Annu Rev Cell Dev Biol. 1996; 12:697–715. [PubMed: 8970741]
32. Ruoslahti E, Pierschbacher MD. Cell. 1986; 44:517–518. [PubMed: 2418980]
33. Ye YP, Bloch S, Xu BG, Achilefu S. J Med Chem. 2006; 49:2268–2275. [PubMed: 16570923]
34. Xie J, Chen K, Lee HY, Xu C, Hsu AR, Peng S, Chen X, Sun S. J Am Chem Soc. 2008; 130:7542–7543. [PubMed: 18500805]
35. Chen XY. Mini-Rev Med Chem. 2006; 6:227–234. [PubMed: 16472190]
36. Dijkgraaf I, Beer AJ, Wester HJ. Front Biosci. 2009; 14:887–899.
37. Alper PB, Hung SC, Wong CH. Tetrahedron Lett. 1996; 37:6029–6032.
38. Tornoe CW, Christensen C, Meldal M. J Org Chem. 2002; 67:3057–3064. [PubMed: 11975567]
39. Kolb HC, Finn MG, Sharpless KB. Angew Chem Int Ed. 2001; 40:2004–2021.
40. Rostovtsev VV, Green LG, Fokin VV, Sharpless KB. Angew Chem Int Ed. 2002; 41:2596–2599.
41. Punna S, Kuzelka J, Wang Q, Finn MG. Angew Chem Int Ed. 2005; 44:2215–2220.
42. Lim EH, Danthi N, Bednarski M, Li KC. Nanomed: Nanotechnol Biol Med. 2005; 1:110–114.
43. Li F, Liu J, Jas GS, Zhang J, Qin G, Xing J, Cotes C, Zhao H, Wang X, Diaz LA, Shi ZZ, Lee DY, Li KC, Li Z. Bioconjugate Chem. 2010; 21:270–278.
44. Nisato R, Tille JC, Jonczyk A, Goodman S, Pepper M. Angiogenesis. 2003; 6:105–119. [PubMed: 14739617]
45. Meldrum T, Schroder L, Denger P, Wemmer DE, Pines A. J Magn Reson. 2010; 205:242–246. [PubMed: 20542715]
46. Pechkovsky DV, Scaffidi AK, Hackett TL, Ballard J, Shaheen F, Thompson PJ, Thannickal VJ, Knight DA. J Biol Chem. 2008; 283:12898–12908. [PubMed: 18353785]
47. Scaffidi AK, Moodley YP, Weichselbaum M, Thompson PJ, Knight DA. J Cell Sci. 2001; 114:3507–3516. [PubMed: 11682610]
48. Scaffidi AK, Petrovic N, Moodley YP, Fogel-Petrovic M, Kroeger KM, Seeber RM, Eidne KA, Thompson PJ, Knight DA. J Biol Chem. 2004; 279:37726–37733. [PubMed: 15187087]
49. Nogales A, García C, Pérez J, Callow P, Ezquerra TA, Gonzalez-Rodríguez J. J Biol Chem. 2010; 285:1023–1031. [PubMed: 19897481]
50. Rivas G, Tangemann K, Minton AP, Engel J. J Mol Recognit. 1996; 9:31–38. [PubMed: 8723317]
51. Schlundt A, Kilian W, Beyermann M, Sticht J, Gunther S, Hopner S, Falk K, Roetzschke O, Mitschang L, Freund C. Angew Chem Int Ed. 2009; 48:4142–4145.
52. Leffler JE, Temple RD. J Am Chem Soc. 1967; 89:5235–5246.
53. Hillman MC, Zolotarjova NI, Patrick DR, McCabe DD, Shen K, Corman JI, Billheimer JT, Seiffert DA, Hollis GF, Wynn R. Protein Expression Purif. 2002; 25:494–502.
54. Spence MM, Ruiz EJ, Rubin SM, Lowery TJ, Winssinger N, Schultz PG, Wemmer DE, Pines A. J Am Chem Soc. 2004; 126:15287–15294. [PubMed: 15548026]

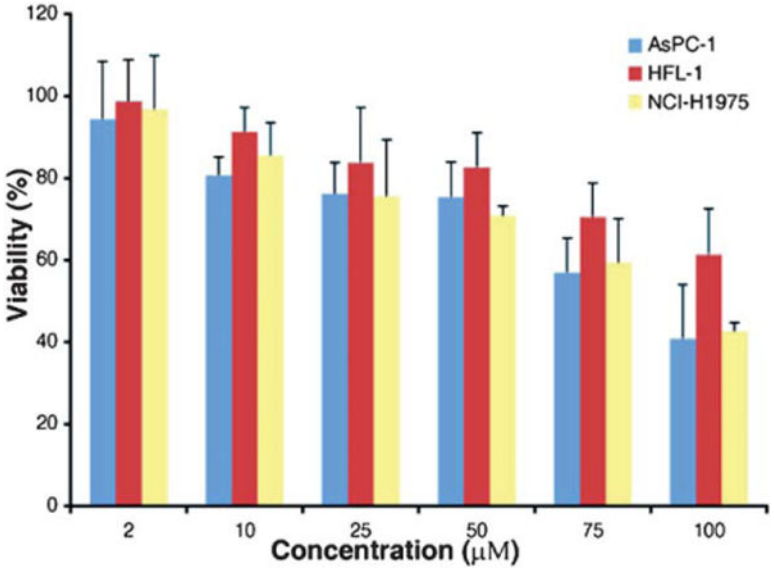

Fig. 1.

Viability of AsPC-1 (blue), HFL-1 (red) and NCI-H1975 (yellow) cells after treatment with increasing concentrations of c[RGDyK]-labeled cryptophane **3**. % Viability was measured by MTT assay after 24 h incubation with increasing concentrations of **3** as compared with untreated cells.

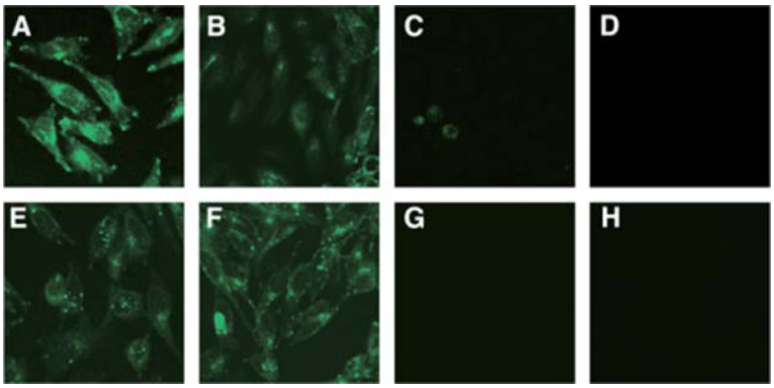

Fig. 2.

Uptake of 1 μM Alexa Fluor 488-labeled c[RGDyK]-cryptophane **4** targeting AsPC-1 cells (A–D) and HFL-1 cells (E–H). Micrographs show **4** uptaken by cells after 1 h incubation (A, E). Targeting of **4** was relatively unaffected by co-incubation with 10 μM c[RADfK] (B, F). However, uptake of **4** was blocked by co-treatment with 10 μM c[RGDyK] peptide (C, G) and 0.15 mg mL^{-1} anti-α_v antibody (D, H).

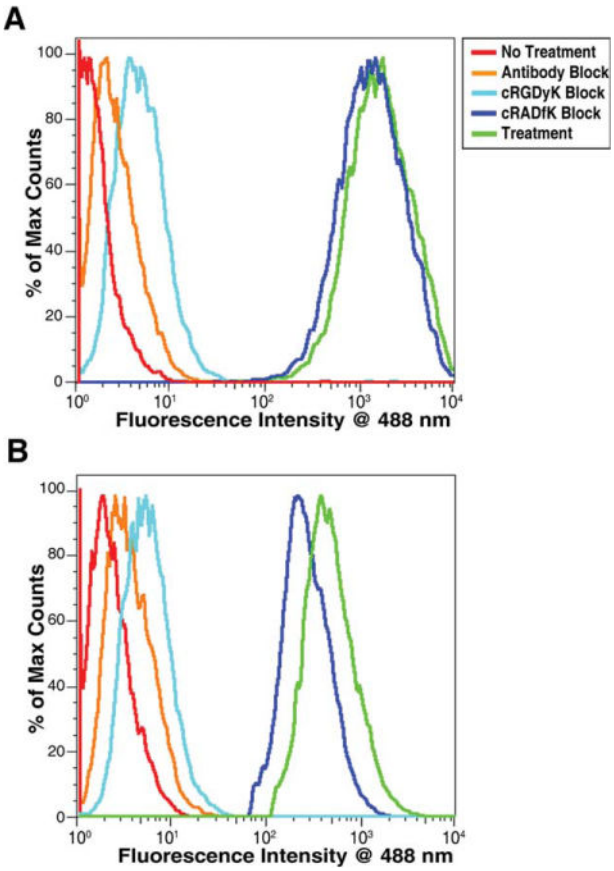

Fig. 3.

Flow cytometry data for (A) AsPC-1 and (B) HFL-1 cells after incubation with 1 μM **4**. Mean fluorescence intensities at 488 nm after treatment with cryptophane were 2100 for AsPC-1 cells (green, in A) and 580 for HFL-1 cells (green, in B). Mean fluorescence intensities for all conditions are listed in Table S1 of the supporting information.†

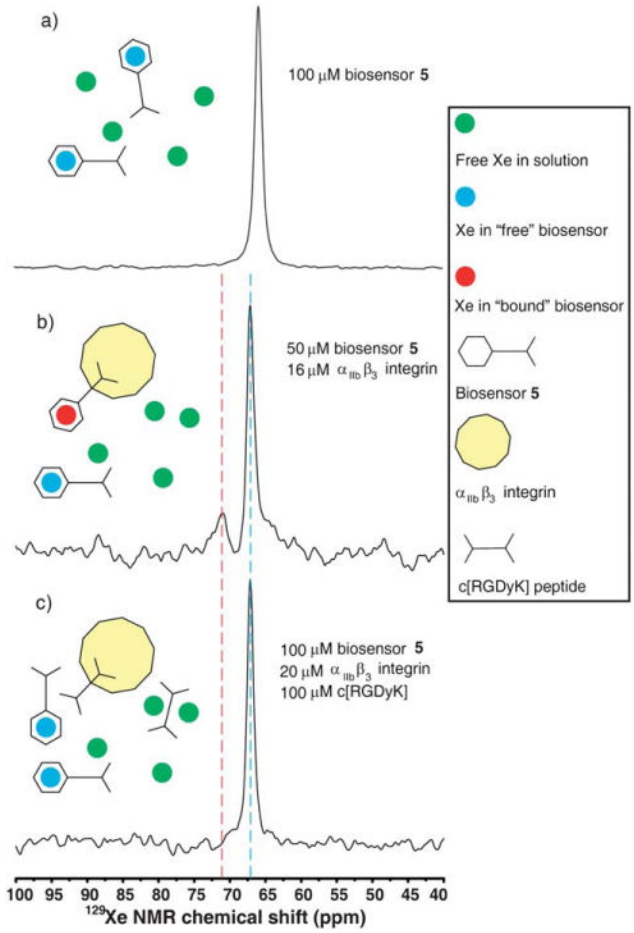

Fig. 4.

Hyperpolarized ^{129}Xe NMR spectra of biosensor **5** alone, binding $\alpha_{IIb}\beta_3$ integrin, and blocked by c[RGDyK], all studies in Tris buffer (1 mM, pH 7.2) (a) **5** gave ^{129}Xe NMR chemical shift at 65.8 ppm. (b) **5** and $\alpha_{IIb}\beta_3$ integrin in Tris buffer with 30% glycerol and 0.1% Triton X-100. "Free" biosensor gave ^{129}Xe NMR chemical shift at 67.1 ppm, which was shifted 1.3 ppm downfield from "free" biosensor in (a) due to addition of glycerol. "Bound" biosensor appeared at 71.2 ppm, representing a 4.1 ppm downfield shift. (c) c[RGDyK] added to solution of **5** and $\alpha_{IIb}\beta_3$ integrin gave "free" biosensor at the same ^{129}Xe NMR chemical shift, but no "bound" biosensor was detected.

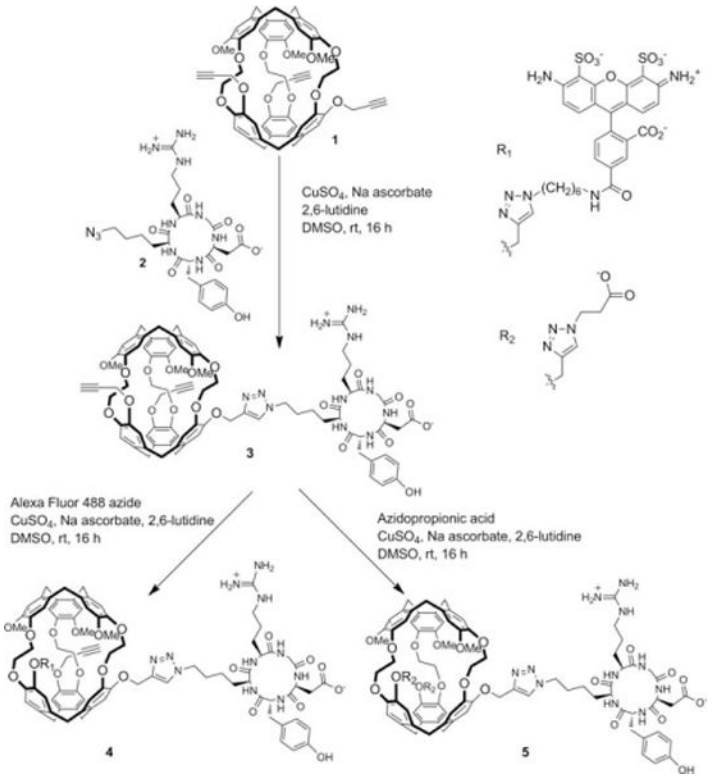

Scheme 1.
Synthesis of c[RGDyK]-labeled cryptophane biosensors.

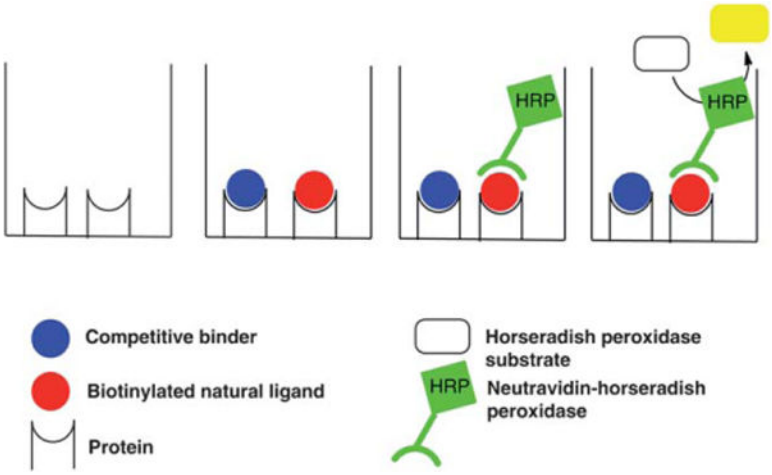

Scheme 2.

In vitro integrin competitive binding assay. One of three integrin proteins ($\alpha_v\beta_3$, $\alpha_{IIb}\beta_3$, $\alpha_v\beta_5$) was coated on a 96 well plate with overnight incubation. Biotinylated natural ligands (red circles) and c[RGDyK]-labeled cryptophane **3** (competitive binder, blue circles) were added to the integrin and incubated for 3 h. Unbound compounds were removed with gentle washing and NeutrAvidin–HRP was added to each well. Bound NeutrAvidin–HRP was then quantified using tetramethyl benzidine horseradish peroxidase substrate.

Table 1

IC_{50} values for biosensor **3** and peptide controls

	IC_{50} (nM)		
	$\alpha_v\beta_3$	$\alpha_{IIb}\beta_3$	$\alpha_v\beta_5$
Biosensor 3	31.6±2.1	18.1±2.4	700
c[RADfK]	>5000	>1000	>10 000
c[RGDyK]	8.2 ± 2.0	1.6 ± 0.6	200